Journal of Structural Chemistry. Vol. 57, No. 1, pp. 167-174, 2016.

CRYSTAL STRUCTURE AND SOME PROPERTIES OF EUROPIUM(III) *CATENA*-{TRIS(1,3-DIETHYL-2-THIOBARBITURATE)}

N. N. Golovnev[1], M. S. Molokeev[2,3], and S. N. Vereshchagin[4]

UDC 541.49:548.73

The $[Eu(HDTBA)_3]_n$ complex (**I**), HDTBA is 1,3-diethyl-2-thiobarbituric acid ($C_8H_{12}N_2O_2S$) is synthesized and its structure is determined by X-ray crystallography. The crystals of **I** are triclinic: a = 11.0205(2) Å, b = 11.8811(3) Å, c = 12.7312(2) Å, α = 100.933(1)°, β = 109.704(1)°, γ = 101.161(1)°, V = 1479.88(5) Å^3, space group P-1, Z = 2. Each of three independent $DETBA^-$ ions is a bridging μ_2-O,O′-coordinated ligand. The coordination polyhedron of Eu(III) is a distorted octahedron. Bridging $DETBA^-$ organize the octahedra into an infinite two-dimensional layer. The structure contains intramolecular hydrogen bonds but intermolecular hydrogen bonds and the π–π interaction are absent. The results of IR spectroscopy and photoluminescence agree with the single crystal X-ray diffraction data. The main product of the thermal decomposition of **I** at 900°C is oxysulfate $Eu_2O_2SO_4$.

DOI: 10.1134/S0022476616010200

Keywords: crystal structure, complex, europium(III), 1,3-diethyl-2-thiobarbituric acid, thermal analysis, IR spectroscopy, photoluminescence.

Lanthanide-based metal-organic hybrid materials exhibit highly monochromatic luminescent radiation, which is applied in clinical diagnostics and biotechnology [1, 2] and in a number of high technology devices [3-5]. Thus, europium oxide has been widely used in TV tubes as an activator of the luminescence of red phosphorus (Eu^{3+}:YVO_4), and Eu-doped Y_2O_3 oxide or Y_2O_2S oxysulfidehave recently been used as red phosphorus. Europium compounds are also exploited in computer monitors, X-ray screens, mercury lamps, neutron scintillators, and charged particle detectors [4, 5].

We have previously synthesized [6] a Eu(III) complex with 2-thiobarbituric acid (H_2TBA) and determined its structure. In this work, in order to study the effect of substituents in H_2TBA on the molecular and supramolecular structure of Eu(III) complexes the structure and some properties of a new Eu(III) complex with N,N′-substituted derivative of H_2TBA – 1,3-diethyl-2-thiobarbituric acid ($C_8H_{12}N_2O_2S$, HDETBA) were investigated. Apart from (Li, Na, K)DETBA [8], data on the structure of metal complexes with HDETBA [7] have been absent at present. Some thiobarbituric acids have been used in medicine under the names sodium thiopental, thiobarbital, and thiobutabarbital [9-11]. Thiobarbituric acids are β-diketones whose complexes with Eu(III) have a high quantum efficiency of photoluminescence and a high thermal stability, which makes them promising materials for, e.g., the production of light emitting diodes [2, 12].

[1]Siberian Federal University, Krasnoyarsk, Russia; ngolovnev@sfu-kras.ru. [2]Kirensky Institute of Physics, Siberian Branch, Russian Academy of Sciences, Krasnoyarsk, Russia. [3]Far Eastern State Transport University, Khabarovsk, Russia. [4]Institute of Chemistry and Chemical Technology, Siberian Branch, Russian Academy of Sciences, Krasnoyarsk, Russia. Translated from *Zhurnal Strukturnoi Khimii*, Vol. 57, No. 1, pp. 171-178, January-February, 2016. Original article submitted February 10, 2015.

EXPERIMENTAL

We used 1,3-diethyl-2-thiobarbituric acid (Sigma-Aldrich, CAS No. 110871-86-8, basic compound ≥ 98%), $Eu(CH_3COO)_3 \cdot 3H_2O$ (chemically pure), NaOH (chemically pure), and KBr (chemically pure).

Synthesis of $Eu(DETBA)_3$ (I). 0.15 g (0.33 mmol) of $Eu(CH_3COO)_3 \cdot 3H_2O$ were dissolved in 10 ml of water, 0.20 g (1.0 mmol) of solid HDETBA were added, and pH of the mixture was brought to 4.5-5.01 with a NaOH solution. After the intensive stirring and grinding of HDETBA lumps the mixture was left for a day, and then the yellow crystalline precipitate was filtered off, washed with acetone, and dried in the air. Single crystals were isolated during the slow evaporation of the filtrate at room temperature. The elemental analysis results for **I** (found/calculated, wt.%): C 39.1/38.45, H 4.62/4.44, N 11.0/11.21, S 12.57/12.83. The product yield was 95 wt. %.

X-ray crystallography. Intensities of X-ray reflections from a crystal with the dimensions of 0.2×0.2×0.2 mm were measured at 296 K on a single crystal SMART APEX II diffractometer with a CCD detector (Bruker AXS), MoK_α radiation, λ = 0.7106 Å. The orientation matrix and cell parameters were determined and refined based on 7161 reflections. The cell corresponded to the triclinic crystal symmetry. Space group *P*-1 was determined from the analysis of the statistics of all reflection intensities. The absorption correction was applied based on the analysis of equivalent reflection intensities. Then the equivalent reflection intensities were averaged and further only independent reflections were used.

The model was solved by direct methods using the SHELX-2014 program package [13]. As a result, the coordinates of all non-hydrogen atoms were found. The asymmetric cell contained an Eu^{3+} ion in general position 2*i* and three $DETBA^-$ ions in general position 2*i*. The obtained structure was refined by the least squares technique using SHELX-2014. Thermal parameters of all non-hydrogen atoms were refined in the anisotropic approximation. Coordinates of hydrogen atoms of the $DETBA^-$ ion were idealized. The analysis of the structure for additional lost symmetry elements and possible voids, which was performed using the PLATON program [14], did not reveal any.

The powder diffraction pattern of the decomposition product of the crystals of **I** was measured at room temperature on a Bruker D8 ADVANCE diffractometer with a VANTEC linear detector and CuK_α radiation. Almost all reflections were indexed by the monoclinic cell (*C*2/*c*) with parameters close to those of $Eu_2O_2SO_4$ [15]. Thus, its structure was used as a starting model in the Rietveld refinement. The refinement was carried out using the TOPAS 4.2 program [16]; it was stable and yielded low divergence factors: R_{wp} = 4.72%, R_p = 3.74%, χ^2 = 1.11, R_B = 1.08% (Fig. 1).

A synchronous thermal analysis was performed on a Netzsch STA Jupiter 449C instrument combined with an Aeolos QMS 403C mass spectral analyzer. The experiments were conducted in a flow of the 20% O_2–Ar mixture in

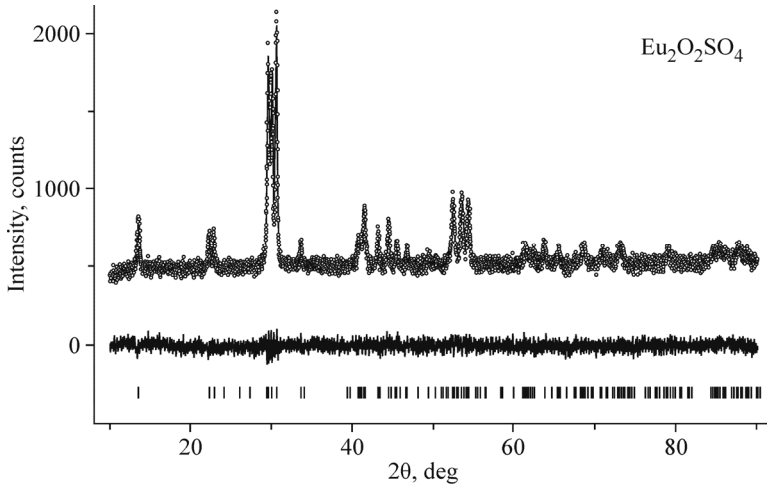

Fig. 1. Experimental (dots), theoretical (line), and difference (the line at the bottom) diffraction patterns of the Rietveld refinement of the decomposition product of the crystal of **I.**

platinum crucibles with perforated caps; the portion weight was 4 mg. The temperature program included a stage of temperature stabilization at 40°C for 30 min, which was followed by heating to 900°C with a rate of 10 deg/min. The qualitative composition of released gases was estimated by a change in the intensity of ions with m/z = 18 (H_2O), 28 (N_2, CO), 30 (NO), 32 (O_2), 44 (CO_2), 60 (COS), and 64(SO_2, SO_3).

Photoluminescence (PL) spectra of the air-dried samples of **I** were measured on an SDL-2 spectrofluorometer (LOMO, Russia) at 77 K. IR spectra of the compounds in KBr were measured in the range 400-4000 cm^{-1} on a FTIR Nicolet 6700 spectrometer.

RESULTS AND DISCUSSION

Crystallographic characteristics and experiment parameters are summarized in Table 1.

The graphical representation of all crystal structures and molecules was made using the DIAMOND program [17]. The structure of **I** has been deposited with the Cambridge Crystallographic Data Center under number 1047007. The data can be obtained at the site www.ccdc.cam.ac.uk/data_request/cif.

The asymmetric unit of complex **I** contains a Eu^{3+} cation and three $DETBA^-$ anions (Fig. 2), two of which have the *cis*-conformation and one has the *trans*-conformation. These designations of different conformations have previously been used in [8]. All $DETBA^-$ ions are coordinated to Eu^{3+} through oxygen atoms, and finally, Eu^{3+} is surrounded by six oxygen atoms (the bond length range is 2.207(2)-2.249(3) Å) forming an octahedron. The octahedra do not directly contact with each other, however, they are united into an infinite two-dimensional layer in the *ac* plane by μ_2-O,O′ bridging $DETBA^-$ ions (Fig. 3).

TABLE 1. Main Crystallographic Characteristics of **I** and Parameters of the Experiment

Crystallographic data	
Chemical formula	$C_{24}H_{33}EuN_6O_6S_3$
M_r	749,70
Space group; Z	P-1; 2
a, b, c, Å	11.0205(2), 11.8811(3), 12.7312(2)
α, β, γ, deg	100.933(1), 109.704(1), 101.161(1)
V, $Å^3$	1479.88(5)
D_x, g/cm^3	1.682
μ, mm^{-1}	2.379
Data collection parameters	
Number of meas. / indep. reflections N_1	18798 / 7161
Number of reflections with $I > 2\sigma(I)$, N_2	6275
Absorption correction	Multiscanning
R_{int}	0,0279
$2\theta_{max}$, deg	56,61
h, k, l	$-14 \rightarrow 11$, $-15 \rightarrow 15$, $-13 \rightarrow 16$
Refinement results	
R / $wR(F^2)$ (over N_1 reflections)	0.0353 / 0.0673
R / $wR(F^2)$ (over N_2 reflections)	0.0269 / 0.0633
S	0.999
Weight scheme	$w = 1/[\sigma^2(F_0^2) + (0.0325P)^2 + 1.2197P]$, where $P = \max(F_0^2 + 2F_c^2)/3$
$(\Delta/\sigma)_{max}$	< 0.028
$\Delta\rho_{max}$ / $\Delta\rho_{min}$, $e/Å^3$	0.777 / –0.799

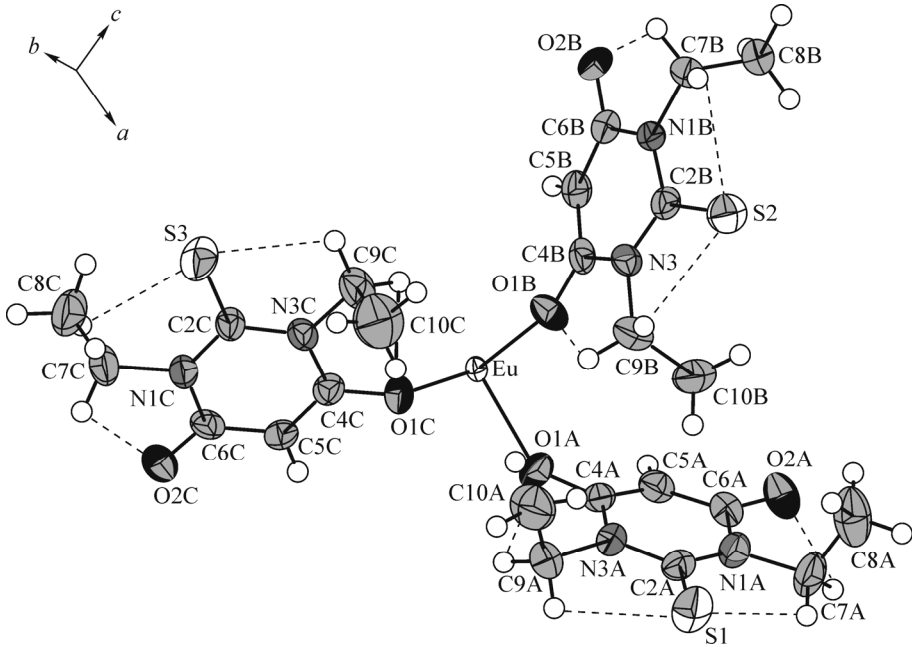

Fig. 2. Asymmetric unit cell of **I**. Intramolecular hydrogen bonds are shown by dashed lines.

Intermolecular hydrogen bonds were not found in the structure. The π–π interactions are also absent because the minimum distance between the centers of the $DETBA^-$ rings is 5.635(2) Å. However, there are weak intramolecular hydrogen bonds [18, p. 52] (Table 2) as in HDETBA compounds [17, 18] and (Li, Na, K)DETBA [8].

A comparison of the structures of **I** and HDETBA with (Li, Na, K)DETBA shows that in (Li, Na, K)DETBA the C2–S bond length is noticeably longer (1.684-1.694 Å) than that in compounds **I** and HDETBA (1.661-1.664 Å) (Table 3). This can be explained by that in (Li, Na, K)DETBA the ligand is coordinated to the metal ion through the S atom while in other compounds this interaction is absent. In its turn the C4–O1 and C6–O2 bond lengths in **I** (1.269-1.281 Å) exceed those

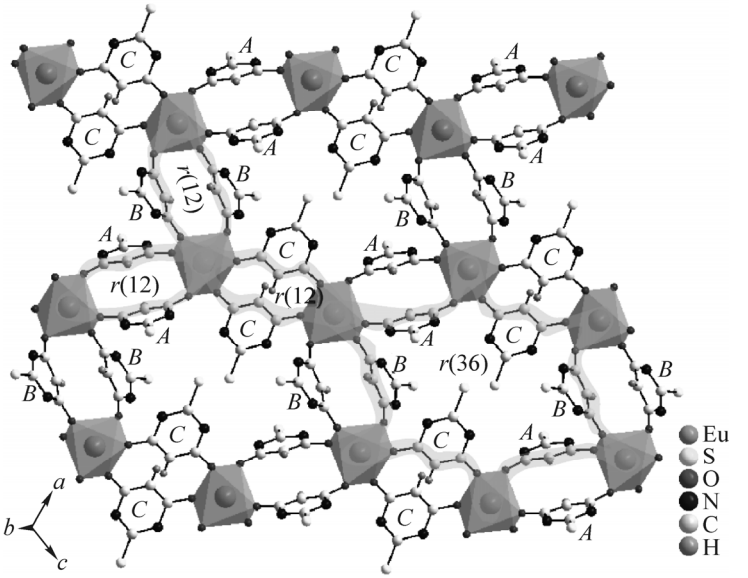

Fig. 3. Structure of the layer formed by octahedra due to bridging $DETBA^-$ in the *ac* plane. To simplify the figure the $–CH_2–CH_3$ groups in $DETBA^-$ ions are omitted. Cyclic structures are marked and designated by the letter *r*; their dimensionality is given in parentheses. The letters *A*, *B*, *C* denote three independent $DETBA^-$ ions.

TABLE 2. D–H···A Hydrogen Bonds (Å, deg) in the Structure of **I**

D–H···A	D–H	H···A	D···A	∠D–H···A
C7*A*–H71*A*···O2*A*	0.97	2.376(3)	2.643(5)	96.4(3)
C7*A*–H72*A*···S1	0.97	2.540(1)	3.006(4)	109.5(3)
C9*A*–H91*A*···S1	0.97	2.5980(12)	2.982(5)	103.8(3)
C9*A*–H92*A*···O1*A*	0.97	2.381(3)	2.704(6)	98.7(2)
C7*B*–H72*B*···O2*B*	0.97	2.362(3)	2.690(6)	98.9(3)
C7*B*–H71*B*···S2	0.97	2.5700(14)	2.985(5)	105.9(3)
C9*B*–H92*B*···S2	0.97	2.5926(13)	2.987(5)	104.5(2)
C9*B*–H91*B*···O1*B*	0.97	2.318(3)	2.654(5)	99.3(2)
C7*C*–H72*C*···O2*C*	0.97	2.330(3)	2.679(6)	100.3(3)
C7*C*–H71*C*···S3	0.97	2.5843(15)	2.986(5)	105.0(2)
C9*C*–H91*C*···S3	0.97	2.5535(11)	2.991(4)	107.4(2)
C9*C*–H92*C*···O1*C*	0.97	2.354(3)	2.685(5)	99.2(3)

in (Li, Na, K)DETBA (1.248-1.270 Å), which can be attributed to a larger formal charge of the Eu^{3+} ion, and consequently, its larger polarizing effect on the C–O bonds as compared with singly charged Li^+, Na^+, and K^+ ions. It should be noted that C4–O1 and C6–O2 bond lengths in HDETBA with a thiomonocarbonyl structure considerably differ from each other [19, 20], but during the formation of compounds (Li, Na, K)DETBA and **I** the metal ion substitutes for the proton in HDETBA and together with the μ_2-O,O′-coordination of $DETBA^-$ they level the electron density in the molecular O1–C4–C5(H)–C6–O2 fragment. This has previously been observed for 2-thiobarbiturate complexes of metals [21].

According to the thermal analysis data in the oxidizing atmosphere, complex **I** is stable up to 250-280°C. At higher temperatures the TG and DSC curves of the thermal decomposition demonstrate three temperature transformation regions (Fig. 4) differing in the sign of the thermal effect and the composition of products.

TABLE 3. Main Geometric Characteristics: Bond Lengths (Å), Bond and Torsion Angles (deg) in MDETBA (M = H, Li, Na, K) and **I**

Parameter	H^+	Li^+	Na^+	Eu^{3+}			K^+
				A	*B*	*C*	
S–C2	1.661	1.684(3)	1.685(3)	1.661(4)	1.664(4)	1.659(4)	1.693(2)
O1–C4	1.264	1.248(3)	1.240(3)	1.278(5)	1.269(5)	1.281(4)	1.254(3)
O2–C6	1.312	1.270(3)	1.258(4)	1.273(3)	1.269(5)	1.273(5)	1.249(2)
N1–C2	1.377	1.373(3)	1.367(4)	1.379(3)	1.376(5)	1.385(5)	1.367(3)
N1–C6	1.375	1.404(3)	1.416(4)	1.387(5)	1.392(5)	1.383(5)	1.425(3)
N3–C2	1.389	1.369(3)	1.354(3)	1.376(5)	1.380(5)	1.380(4)	1.366(3)
N3–C4	1.383	1.416(4)	1.421(4)	1.391(5)	1.388(5)	1.385(5)	1.430(3)
C4–C5	1.399	1.385(4)	1.369(4)	1.367(4)	1.384(5)	1.370(6)	1.380(3)
C5–C6	1.365	1.377(4)	1.381(3)	1.374(5)	1.383(6)	1.377(4)	1.390(3)
S–C2–N1	122.6	121.4(2)	120.7(2)	122.2(3)	122.1(3)	121.7(3)	122.2(1)
S–C2–N3	122.0	121.6(2)	122.1(2)	121.7(3)	121.6(3)	122.0(3)	120.4(1)
N1–C2–N3	115.4	116.9(2)	117.3(2)	116.1(3)	116.2(3)	116.3(3)	117.4(2)
C4–C5–C6	119.4	122.9(2)	123.1(2)	121.7(4)	121.2(3)	121.8(3)	123.3(2)
C2–N1–C7–C8	–87.0	–84.9(3)	–88.8(3)	–96.1(5)	–90.5(4)	88.5(4)	89.5(2)
C2–N3–C9–C10	88.2	84.8(3)	88.2(4)	89.4(4)	89.3(4)	90.4(5)	88.0(2)
Conformation	*cis*	*cis*	*cis*	*cis*	*cis*	*trans*	*trans*
Reference	[19, 20]	[8]	[8]	[This work]	[This work]	[This work]	[8]

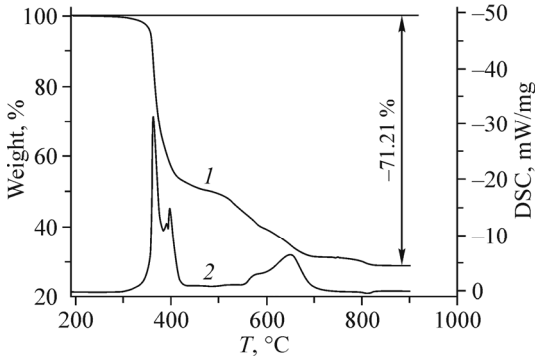

Fig. 4. TG (*1*) and DSC (*2*) curves for the oxidizing decomposition of **I.**

At the first stage, which started at about 280°C and proceeded with a high heat release, the weight loss was accompanied by the appearance of ions with *m*/*z* 18, 30, 44, 60, and 64 in the mass spectrum (Fig. 5). It is most likely that in this temperature range the oxidizing decomposition of the organic component of the salt occurs with the formation of gaseous oxidation products (CO_2, H_2O, NO, COS, SO_2) along with the carbonization of the unreacted part; the weight loss in this region is about 51%.

At the second, also exothermic stage at 450-750°C there is additional oxidation of the carbonized residue containing considerable amounts of sulfur and nitrogen but practically no hydrogen (Fig. 5*A* and *B*). The weight loss at the last endothermic stage of the transformation is accompanied by an increase in the intensity of the ion with *m*/*z* = 64 (Figs. 4, 5*B*). The release of SO_2 in it at 750-900°C is most likely to correspond to the decomposition of Eu(III) sulfate (Eq. 1) occurring at about 800°C [22]. The total weight loss (Δm) on heating **I** to 900°C is 71.21%, which is well consistent with the theoretical value for process (2)

$$Eu_2(SO_4)_3 \rightarrow Eu_2O_2SO_4 + 2SO_2 + O_2, \quad (1)$$

$$Eu(DETBA)_3 \rightarrow 1/2Eu_2O_2SO_4 \cdot \Delta m = 71.19\%. \quad (2)$$

Oxysulfates $Ln_2O_2SO_4$ have a great capacity with respect to oxygen atoms [22] and are promising as catalysts resistive to sulfur poisoning in the reaction of producing hydrogen from CO and H_2O [23]. The thermal decomposition of **I** is a new way to obtain $Eu_2O_2SO_4$.

Fig. 6 depicts the PL spectra at 77 K of air-dried **I** and the $Eu_2O_2SO_4$ product of its thermal decomposition which were obtained by excitation at 273 nm (the most intense band in the excitation spectrum). At room temperature no luminescence is observed in the samples. The PL spectra are due to the *f*–*f* luminescence of Eu(III). The bands observed for **I** and $Eu_2O_2SO_4$ completely coincide in the range 500-750 nm. An intense line at 620 nm corresponds to the electron dipole

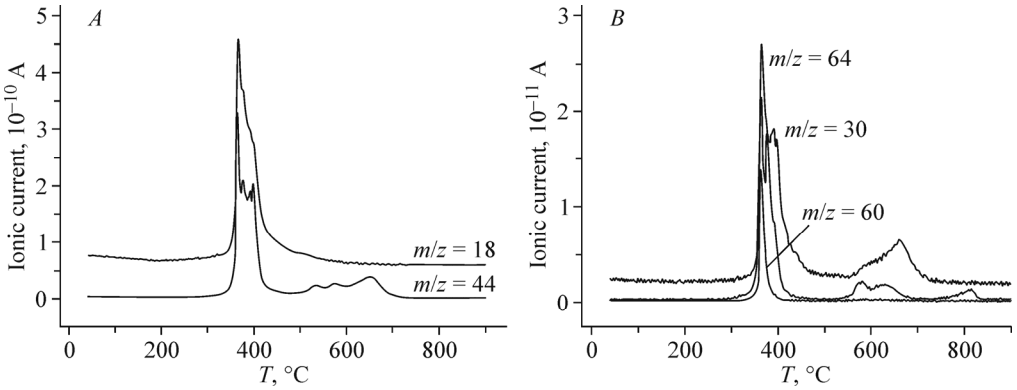

Fig. 5. Mass spectral intensities of ions with *m*/*z* 18, 30, 44, 60, and 64 for the oxidizing decomposition process of **I.**

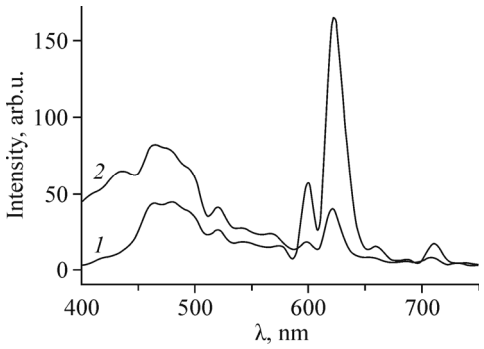

Fig. 6. Photoluminescence spectra of $Eu(DETBA)_3$ (*1*) and $Eu_2O_2SO_4$ (*2*).

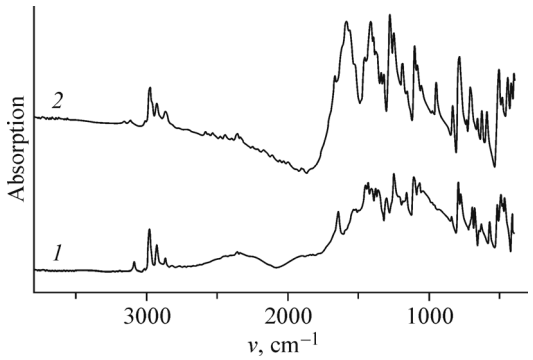

Fig. 7. Survey IR spectra of HDETBA (*1*) and **I** (*2*).

transition $^5D_0 \rightarrow {}^7F_2$ [3, 24]. Weakly intense bands at 710 nm and 600 nm are assigned to $^5D_0 \rightarrow {}^7F_4$ and $^5D_0 \rightarrow {}^7F_1$ transitions respectively. The absence of the electron dipole $^5D_0 \rightarrow {}^7F_0$ transition at 577-581 nm is consistent with the high O_h symmetry of the Eu(III) complex determined by X-ray crystallography. The intensity of the $^5D_0 \rightarrow {}^7F_2$ transition band is much higher than that of $^5D_0 \rightarrow {}^7F_1$, i.e. the Eu^{3+} ion is not located in the center of inversion. It should be noted that the luminescent emission corresponding to the above transitions is applied in light engineering, quantitative and qualitative analysis, and luminescent imaging [3, 5].

In the IR spectrum of crystalline HDETBA (Fig. 7) the intense band at 1646 cm^{-1} was previously assigned to the ν(C=O) vibration [17]. Along with it, in the IR spectrum of **I** in the ν(C=O) vibrational region three intense bands appeared at 1667 cm^{-1}, 1587 cm^{-1}, and 1563 cm^{-1}, which indicate the ligand coordination through the oxygen atom. As in the case of 2-thiobarbituric acid [25], the strong band at 1160 cm^{-1} in the IR spectra of HDETBA and **I** can be assigned to ν(C=S) vibrations. The permanent position and intensity of this band agrees with the absence of $DETBA^-$ coordination through S atoms. Thus, the IR spectroscopic results indirectly confirm the X-ray crystallographic data.

The work was supported within the State Contract of the Ministry of Education and Science of the Russian Federation for research in the Siberian Federal University in 2015.

REFERENCES

1. M. C. Heffen, L. M.Matosziuk, and T. J. Meade, *Chem. Rev*., **114**, No. 8, 4496-4539 (2014).
2. Y. Yang, Q. Zhao, W. Feng, and F. Li, *Chem. Rev*., **113**, No. 1, 192-270 (2013).
3. S. Cotton, *Lanthanide and Actinide Chemistry*, Wiley, Uppingham, Rutland, UK (2006).
4. J. Rocha, L. D. Carlos, F. A. A. Paz, and D. Ananias, *Chem. Soc. Rev*., **40,** 926-940 (2011).
5. K. Binnemans, *Chem. Rev*., **109**, No. 9, 4283-4374 (2009).
6. N. N. Golovnev and M. S. Molokeev, *Koord. Khim*., **40**, No. 9, 564-568 (2014).
7. *Cambridge Structural Database. Version 5.35*, University of Cambridge, UK (2013).
8. N. N. Golovnev, M. S. Molokeev, S. N. Vereshchagin, et al., *Polyhedron*, **85,** 493-498 (2015).
9. M. D. Mashkovskii, *Drugs: Handbook for Doctors* [in Russian], RIA Novaya volna, Moscow (2008).
10. R. Dawson, D. Elliot, W. Elliot, and K. Jones, *Data for Biochemical Research*, Clarendon Press, Oxford (1986).
11. F. H. Bamanie, A. S. Shehata, M. A. Moustafa, and M. M. Mashaly, *J. Am. Sci*., **8**, No. 1, 481-485 (2012).
12. H. Tian, R. Tang, and M. Zhao, *ECS J. Solid State Sci. Technol*., **2**, No. 3, 33-38 (2013).
13. G. M. Sheldrick, *Acta. Crystallogr*., **A64**, No. 1, 112-122 (2008).
14. *PLATON – A Multipurpose Crystallographic Tool*, Utrecht University, Utrecht, The Netherlands (2008).
15. *TOPAS V4: General Profile and Structure Analysis Software for Powder Diffraction Data, User's Manual*, Bruker AXS, Karlsruhe, Germany (2008).

16. I. Hartenbach and T. Schleid, *Z. Anorg. Allg. Chem*., **628,** 2171 (2002).
17. K. Brandenburg and M. Berndt, *DIAMOND – Visual Crystal Structure Information System*, Crystal Impact GbR, Bonn, Germany (1999).
18. J. W. Steed and J. L. Atwood, *Supramolecular Chemistry*, Wiley, Chichester (2000).
19. J. P. Bideau, P. V. Huong, and S. Toure, *Acta Crystallogr*., **B32**, No. 2, 481/482 (1976).
20. J. P. Bideau, P. V. Huong, and S. Toure, *Acta Crystallogr*., **B33**, No. 12, 3847-3849 (1977).
21. N. N. Golovnev and M. S. Molokeev, *2-Thiobarbituric Acid and Its Complexes with Metals: Synthesis, Structure, and Properties* [in Russian], Sib. Fed. Univ., Krasnoyarsk (2014).
22. M. Machida, K. Kawamura, K. Ito, and K. Ikeue, *Chem. Mater*., **17**, No. 6, 1487-1492 (2005).
23. I. Valsamakis and M. Flytzani-Stephanopoulos, *Appl. Catal*., **B106,** 255-263 (2011).
24. B. V. Bukvetskii, A. G. Mirochnik, P. A. Zhikhareva, and V. E. Karasev, *J. Struct. Chem*., **51**, No. 6, 1164-1169 (2010).
25. E. Mendez, M. F. Cerda, J. S. Gancheff, et al., *J. Phys. Chem*., **C111**, No. 8, 3369-3383 (2007).